

STRUCTURAL AND OPTICAL PROPERTIES OF NANOCRYSTALLINE $\text{Cu}_x\text{Cd}_{1-x}\text{S}$ THIN FILMS DEPOSITED BY CHEMICAL BATH DEPOSITION TECHNIQUE

J. F. MOHAMMAD

University of Anbar, College of education for pure Sciences, Physics Department, Iraq

Due to the importance of this field and its applications, especially in the field of solar cells, studies are still ongoing to study the physical properties of nanostructure materials. Using chemical bath deposition (CBD) technique, nanocrystalline copper-cadmium-sulfide ($\text{Cu}_x\text{Cd}_{1-x}\text{S}$) thin films were synthesized from a mixture of copper chloride, cadmium chloride and thiourea. The X-ray diffraction (XRD) pattern confirms that the deposited thin films are polycrystalline in nature with hexagonal phase. The intensity decreases as Cu^{2+} content in the solution increase. Atomic force microscopy (AFM) was used to investigate surface morphology characterization, which showed that the films have a nanocrystalline structure in the range of 5–11 nm and that surface morphology is affected by Cu^{2+} content in the bath solution. The optical properties were investigated using UV-VIS spectrophotometer in the range of 300-1100 nm. Optical analysis showed that band gap increases from 3.77 to 3.96 eV as Cu^{2+} content increase in chemical bath solution from $x=0.1$ to $x=0.5$

(Received November 28, 2017; Accepted March 5, 2018)

Keywords: Chalcogenide, Chemical Bath, XRD, CdS and CuS thin films, Bandgap

1. Introduction

Recently, nanocrystalline materials have unveiled a new horizon in the field of electronic applications, since the material properties could be varied according to the crystallite size and/or thickness of the film variation [1]. Synthesis of nanostructured composite chalcogenide materials have grabbed a great interest in scientific research because of its photovoltaic application [2]. Some applications of the current material science require the creation of a new ternary and quaternary semiconductor materials whose physical and chemical properties can be controlled to obtain unique electronic and optical properties (for example CdZnS and CdCuS), depending on the content of Zn, Cd and Cu and preparation conditions such as temperature, time and PH etc. [3-7]. Optical and electrical properties of chalcogenides have many applications in solar selective coatings, photovoltaic devices, IR detectors and electro-optic modulators[8]. CuS and CdS thin films have been prepared by different techniques such as spray pyrolysis [9,10], successive ionic layer adsorption and reaction (SILAR) [11], electrodeposition [12,13] and chemical bath deposition (CBD) [14-16]. The chemical bath deposition (CBD) method has become very popular recently, especially for the metal chalcogenide thin film deposition, because it is simple, convenient for large area deposition and less expensive than other thin film deposition methods which allow for manufacturing relatively low cost devices [17,18]. The aim of this work is to synthesize nanocrystalline $\text{Cu}_x\text{Cd}_{1-x}\text{S}$ thin films and study their structural and optical properties for solar cell applications.

2. Experimental

Commercially available glass slide substrate has been employed in this work. The substrates were washed ultrasonically for 10 minutes using clean beaker containing ethanol and distilled water and then dried by an air-jet. For the preparation of nanocrystalline $\text{Cu}_x\text{Cd}_{1-x}\text{S}$ thin films, Copper chloride (CuCl_2), Cadmium chloride (CdCl_2) and thiourea ($\text{CS}(\text{NH}_2)_2$) were used as the sources of Cu^{2+} , Cd^{2+} and S^{2-} ions respectively. The solution of $\text{Cu}_{0.1}\text{Cd}_{0.9}\text{S}$ was prepared by mixing 4 ml of 0.1M (CuCl_2) with 36 ml 0.1M (CdCl_2) under continuous stirring at room temperature. Aqueous ammonia (NH_4OH) was added to make the solution alkaline and maintain a pH of 10, then 40 ml of 0.2M ($\text{CS}(\text{NH}_2)_2$) was added to the mixture and the substrate was immediately immersed in the beaker containing the solution. The bath temperature was fixed at 65 ± 2 °C, over a deposition time of 120 minutes. The details of three different bath compositions are summarized in Table 1.

Table 1: Details of three different bath compositions of $\text{Cu}_x\text{Cd}_{1-x}\text{S}$ thin films

Sample	CuCl_2 (ml)	CdCl_2 (ml)	$\text{CS}(\text{NH}_2)_2$ (ml)	pH	Time (min.)	Temperature (°C)
$\text{Cu}_{0.1}\text{Cd}_{0.9}\text{S}$	4	36	40	10	120	65 ± 2
$\text{Cu}_{0.3}\text{Cd}_{0.7}\text{S}$	12	28	40	10	120	65 ± 2
$\text{Cu}_{0.5}\text{Cd}_{0.5}\text{S}$	20	20	40	10	120	65 ± 2

3. Results and discussion

3.1. Structural Properties

X-ray diffraction pattern of the prepared $\text{Cu}_x\text{Cd}_{1-x}\text{S}$ thin films (for $x = 0.1, 0.3$ and 0.5) is presented in Figure 1. The presence of diffraction peaks indicates that the film is polycrystalline with a hexagonal structure with preferential orientation along (002) at 26.8° and no amorphous phase is detected. The crystallinity of the films decreased as the quantity of Copper chloride increases in the bath solution, which leads to broadening of the X-ray diffraction spectra and reduction in the crystallite size. Also, it can be observed (figure 1 a) that the existence of two peaks along (110) and (112) which is belonging to the hexagonal structure of cards rather than of course can be explained by the fact that cadmium ions dominant in the reaction process. The decrease in the intensity and increase in full width at half maxima with small shift toward larger 2θ is attributed to the substitution of Copper ions into the Cadmium chloride lattice. Table 2 summarizes the results of crystallite size values which were calculated by using Debye-Scherrer formula (equation 1) according to the FWHM of the predominant peak of each sample [19].

$$D_{hkl} = \frac{K \lambda}{\beta \cos \theta} \quad (1)$$

Where:

D_{hkl} - Crystalline size.

$\lambda = 1.54 \text{ \AA}$ (is the wavelength of X-ray).

$K = 0.94$ (is a constant)

β - Full width at half maximum (FWHM) intensity (rad.)

θ - Bragg's angle.

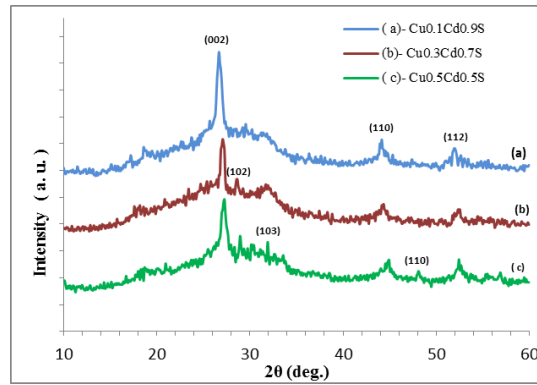


Fig. 1. XRD spectra of nanocrystalline $Cu_xCd_{1-x}S$ thin films
(a): $Cu_{0.1}Cd_{0.9}S$, (b): $Cu_{0.3}Cd_{0.7}S$ and (c): $Cu_{0.5}Cd_{0.5}S$

Table 2. XRD data of nanocrystalline $Cu_xCd_{1-x}S$ thin films.

Sample	2θ (degree)	d-Spacing	hkl	Grain size (nm)
$Cu_{0.1}Cd_{0.9}S$	26.68	3.33041	002	11
$Cu_{0.3}Cd_{0.7}S$	26.78	3.32519	002	7
$Cu_{0.5}Cd_{0.5}S$	27.2	3.27122	002	6

Some applications require thin films to be homogeneous and uniform, especially in solar cell applications. Morphological analysis is carried out using atomic force microscope in order to obtain information about surface formation. Figure 2 shows AFM images in two and three dimensions. It also indicates how the grains are distributed regularly on the surface without surface defects and cracks. From AFM images, the surface texture results of the prepared nanocrystalline $Cu_xCd_{1-x}S$ thin films (for $x=0.1, 0.3$ and 0.5) were listed in Table 3. As the value of x increases from $x=0.1$ to $x=0.5$, a slight decrease in roughness of the film may be occurring due to the decrease in film thickness which lead to a decrease in grain size in nanoscale. Accordingly, it can be suggested that these thin films can be used as a window in solar cells, especially at low concentrations of copper chloride in the bath solution.

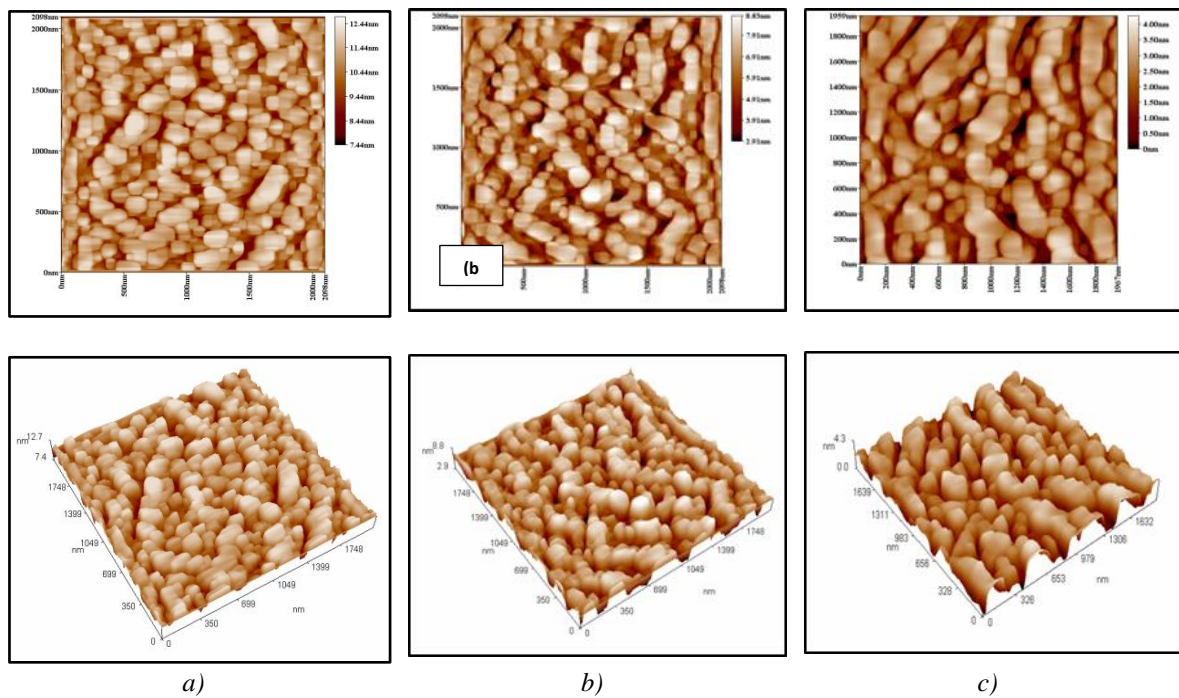


Fig. 2. AFM images of nanocrystalline thin films with 2 dimensional and 3 dimensional of: (a) $\text{Cu}_{0.1}\text{Cd}_{0.9}\text{S}$, (b) $\text{Cu}_{0.3}\text{Cd}_{0.7}\text{S}$ and (c) $\text{Cu}_{0.5}\text{Cd}_{0.5}\text{S}$

Table 3: The calculated surface texture values of the prepared samples.

Sample	Roughness average (nm)	Root mean square (nm)	Ten point height (nm)	Average grain size (nm)
$\text{Cu}_{0.1}\text{Cd}_{0.9}\text{S}$	0.986	1.22	5.9	11
$\text{Cu}_{0.3}\text{Cd}_{0.7}\text{S}$	0.721	0.892	4.41	7
$\text{Cu}_{0.5}\text{Cd}_{0.5}\text{S}$	0.701	0.859	3.92	5

3.2. Optical Properties

The optical properties of the $\text{Cu}_x\text{Cd}_{1-x}\text{S}$ thin films deposited on a glass substrate by the CBD technique at a bath temperature 65 ± 2 have been investigated by the transmission spectra at room temperature. They were measured in the range of 300- 1100 nm. Figure 3 shows the transmittance spectra of the $\text{Cu}_x\text{Cd}_{1-x}\text{S}$ thin films with different Cu-contents ($x=0.1, 0.3$ and 0.5). It is observed that the average transmittance in the visible wavelength region is greater than (80 % for $x=0.5$). As x -content increase in the mixture solution of the bath, the optical transmission spectra increases as a result of the increase of the contribution of copper ions comparing with cadmium ions in the solution which leads to the formation of $\text{Cu}_x\text{Cd}_{1-x}\text{S}$ thin film with high transmittance. The increase in transmittance may be denoted the decrease in film thickness. This feature makes these films applications for optoelectronic devices.

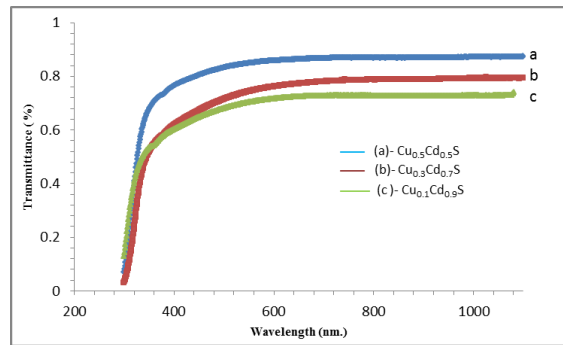


Fig. 3. Transmittance of nanocrystalline $\text{Cu}_x\text{Cd}_{1-x}\text{S}$ thin films

The relationship between the absorption coefficient (α), absorbance (A) and the film thickness (t) is given by [20]:

$$\alpha = \frac{2.3026 A}{t} \quad (2)$$

Fig. 4 shows the absorption coefficient (α) of the $\text{Cu}_x\text{Cd}_{1-x}\text{S}$ thin films with different Cu-contents determined from absorbance measurements using equation (2). The absorption coefficient

of $\text{Cu}_x\text{Cd}_{1-x}\text{S}$ thin films decreases sharply in the UV/VIS boundary, and then decreases gradually in the visible region. It is clear that the films have a low absorption coefficient in the visible region with the shift of the absorption edge to the shorter wavelength (blue shift) with the increase of Cu-content as a result of the quantum confinement effect which is related to the nanosize.

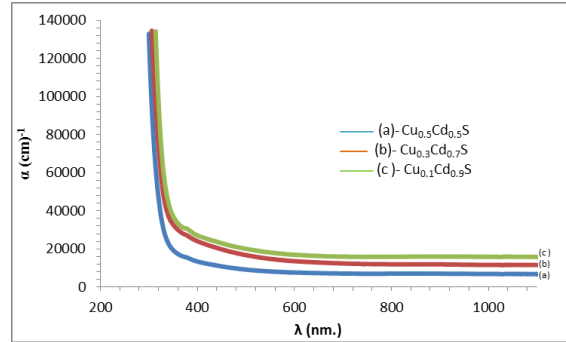


Fig. 4. Absorption spectra of nanocrystalline $\text{Cu}_x\text{Cd}_{1-x}\text{S}$ thin films

The optical band gap (E_g) of the $\text{Cu}_x\text{Cd}_{1-x}\text{S}$ thin films for allowing direct transitions was calculated using the following equation:

$$\alpha h\nu = A (h\nu - E_g)^n \quad (3)$$

Where A is a constant, the best linear fit is obtained for $n = 1/2$. The relations are plotted between $(\alpha h\nu)^2$ and photon energy ($h\nu$), as shown in figure (5) which illustrates allowed direct electronic transition. From figure 5 we can conclude that the band gap of the $\text{Cu}_x\text{Cd}_{1-x}\text{S}$ thin films depends on the Cu-content and E_g increase as x increase. The band gap values of the synthesized nanocrystalline $\text{Cu}_x\text{Cd}_{1-x}\text{S}$ thin films are 3.77, 3.86 and 3.96 eV which correspond to $x = 0.1$, 0.3 and 0.5, respectively. As a comparison, the obtain values are greater than the bulk value of CdS (or CuS) and this indicates the formation of nanoparticles of $\text{Cu}_x\text{Cd}_{1-x}\text{S}$ thin films.

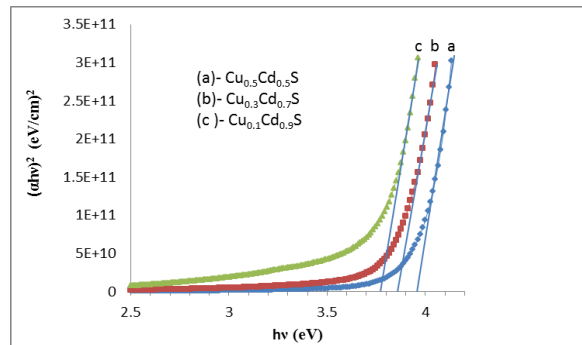


Fig. 5. Optical energy gap of nanocrystalline $\text{Cu}_x\text{Cd}_{1-x}\text{S}$ thin films.

4. Conclusions

Nanocrystalline $\text{Cu}_x\text{Cd}_{1-x}\text{S}$ thin films are successfully deposited by chemical bath deposition technique on glass substrate. The results showed that the prepared films have a polycrystalline nature with a nanocrystalline grains which cover the substrate surface without any cracks, and that the films have a low roughness. The optical transmittance and the energy gap of $\text{Cu}_x\text{Cd}_{1-x}\text{S}$ thin films seem to be influenced by Cu-content in the bath solution and both increase as x increases. The obtained values of E_g were 3.77, 3.86 and 3.96 eV corresponding to $x = 0.1$, 0.3

and 0.5, respectively. The above properties enable researchers to use these thin films in optical applications, especially in solar cells as a window layer.

References

- [1] S. M. Pawar, B. S. Pawar, J. H. Kim, Oh-Shim Joo, C. D. Lokhande, *Current Applied Physics*, **11**, 117 (2011).
- [2] A. U. Ubale, K. S. Chipade, M. V. Bhute, P. P. Raut, G. P. Malpe, Y. S. Sakhare, M. R. Belkhedkar, *International Journal of Materials and Chemistry*, **2**, 165 (2012).
- [3] I. O. Oladeji, L. Chow, *Thin Solid Films*, **474**, 77 (2005).
- [4] C. Jin, W. Zhong, X. Zhang, Y. Deng, C. Au, Y. Du, *Crystal Growth and Design* **9**, 4602 (2009).
- [5] F. Benkabou, H. Aourag, M. Certier, *Materials Chemistry and Physics*, **66**, 10 (2000).
- [6] N. A. Noor, N. Ikram, S. Ali, S. Nazir, S. M. Alay, A. Shaukat, *Journal of Alloys and Compounds*, **507**, 356 (2010).
- [7] S. A. Al Kuhaimi, Z. Tulbah, *J. Electrochem. Soc.*, **147**, 214 (2000).
- [8] C. D. Lokhande, *Mater. Chem. Phys.*, **26**, 405 (1990).
- [9] T. Elango, V. Subramanian, K. R. Murali, *Surf. Coat. Technol.* **123**, 8 (2000).
- [10] A. A. Yadav, M. A. Barote, E. U. Masumdar, *Materials Chemistry and Physics* **121**, 53 (2010).
- [11] B. Guzeldir, M. Saglam, A. Ates, *Acta Physica Polonica*, **121**, 33 (2012).
- [12] M. Izaki, T. Shinagawa, K. Mizuno, Y. Ida, M. Inaba, A. Tasaka, *Journal of Physics D: Applied Physics*, **40**, 3326 (2007).
- [13] A. V. Kokate, U. B. Suryavanshi, C. H. Bhosale, *Sol. Energy*, **80**, 156 (2006).
- [14] S. S. Kale, C. D. Lokhande, *Mater. Chem. Phys.*, **62**, 103 (2000).
- [15] A. S. Khomane, P. P. Hankare, *J. Alloys Comp.*, **489**, 605 (2010).
- [16] S. A. Kumar, M. Swati, T. G. See, *Austin Chemical Engineering*, **1** (1), 1 (2014).
- [17] M. Ashokkumar, S. Muthukumaran, *Physics Procedia*, **49**, 137 (2013).
- [18] R. S. Mane, C. D. Lokhande, *Materials Chemistry and Physics*, **65**, 1 (2000).
- [19] A. U. Ubale, V. S. Sangawar, D. K. Kulkarni, *Bull. Mater. Sci.*, **30**, 147 (2007).
- [20] J. P. Borah, K. C. Sarma, *Acta Physica Polonica A*, **114**, 715 (2008).